

REPORT DOCUMENTATION PAGE

AFRL-SR-BL-TR-02-

Public reporting burden for this collection of information is estimated to average 1 hour per response, including gathering and maintaining the data needed, and completing and reviewing the collection of information. Send collection of information, including suggestions for reducing this burden, to Washington Headquarters Service, Paperwork Project, Suite 1204, Arlington, VA 22202-4302, and to the Office of Management and Budget, Paperwork Project, Suite 1204, Arlington, VA 22202-4302.

Jrces,
of this
erson

1. AGENCY USE ONLY (Leave blank)	2. REPORT DATE 19/07/01	3. REPORT TYPE AND DATES COVERED FINAL (5/1/96 - 4/30/01)
4. TITLE AND SUBTITLE MODELING , ANALYSIS AND DESIGN OF SMART COMPOSITE STRUCTURES AND CURVED ACTUATORS		5. FUNDING NUMBERS F49620-96-1-0195
6. AUTHOR(S) ADITI CHATTOPADHYAY DAN DRAGOMIR		
7. PERFORMING ORGANIZATION NAME(S) AND ADDRESS(ES) ARIZONA STATE UNIVERSITY DEPARTMENT OF MECHANICAL AND AEROSPACE ENGINEERING TEMPE, ARIZONA 85287-6106		8. PERFORMING ORGANIZATION REPORT NUMBER XAA 0014/TE
9. SPONSORING/MONITORING AGENCY NAME(S) AND ADDRESS(ES) AIR FORCE OFFICE OF SCIENTIFIC RESEARCH 801 NORTH RANDOLPH STREET ROOM 732 ARLINGTON, VA 22203-1977		10. SPONSORING/MONITORING AGENCY REPORT NUMBER
11. SUPPLEMENTARY NOTES		
AIR FORCE OFFICE OF SCIENTIFIC RESEARCH (AFOSR) NOTICE OF TRANSMITTAL DTIC. THIS TECHNICAL REPORT HAS BEEN REVIEWED AND IS APPROVED FOR PUBLIC RELEASE LAW AFR 190-12. DISTRIBUTION IS UNLIMITED.		
12a. DISTRIBUTION AVAILABILITY STATEMENT UNLIMITED DISTRIBUTION STATEMENT A Approved for Public Release Distribution Unlimited		12b. DISTRIBUTION CODE
13. ABSTRACT (Maximum 200 words) A general framework has been developed for the analysis of laminated smart structures with embedded and/or surface bonded piezoelectric actuators and sensors. The theory addresses the following issues: (i) accurate description of transverse shear effect in the laminated structural model, (ii) presence of multiple delaminations and (iii) characterization of delamination placement and size on dynamic characteristics. The mathematical model has been implemented using finite element method and extensive numerical investigations have been performed to validate the model with three-dimensional results and available experimental data. Results indicate that the presence of delaminations affect the modal strain distributions in smart composite laminates. The developed theory has been used to characterize delaminations in smart composite plates of arbitrary thickness and results indicate that dynamic strain is a better indicator of damage than frequencies or mode shapes. Significant differences are noted in the RMS values of the response, calculated using modal strain, indicating the presence of damage. A control system has also been designed to minimize the effect of damage. New damage indices based on modal strain are proposed and show promising results.		
14. SUBJECT TERMS		15. NUMBER OF PAGES 17
20020315 087		16. PRICE CODE
17. SECURITY CLASSIFICATION OF REPORT UNCLASSIFIED	18. SECURITY CLASSIFICATION OF THIS PAGE UNCLASSIFIED	19. SECURITY CLASSIFICATION OF ABSTRACT UNCLASSIFIED
20. LIMITATION OF ABSTRACT		

**MODELING, ANALYSIS AND DESIGN OF SMART COMPOSITE
STRUCTURES**

FINAL PROGRESS REPORT

July 19, 2001

Aditi Chattopadhyay – Principal Investigator

Dan Dragomir-Daescu – Graduate Research Associate

Haozhong Gu – Post Doctoral Fellow

Dr. Changho Nam – Visiting Faculty

Department of Mechanical and Aerospace Engineering

Arizona State University

Tempe, AZ 85287-6106

AIRFORCE OFFICE OF SCIENTIFIC RESEARCH

Grant Number: (F49620-96-1-0195 P0004AAH04)

APPROVED FOR PUBLIC RELEASE

DISTRIBUTION UNLIMITED

THE VIEWS, OPTIONS, AND/OR FINDINGS CONTAINED IN THIS REPORT ARE THOSE OF THE AUTHOR(S) AND SHOULD NOT BE CONSTRUED AS AN OFFICIAL DEPARTMENT OF THE ARMY POSITION, POLICY, OR DECISION, UNLESS SO DESIGNATED BY OTHER DOCUMENTATION.

1. Objectives

The objectives of the research were as follows.

- (1) Develop an accurate and general framework of smart composite structures including
 - Accurate representation of through the thickness shear deformation.
 - Presence of multiple delaminations.
 - Two-way coupling between electrical, mechanical and thermal fields in the constitutive relations
- (2) Investigate the use of dynamic strain and RMS values in damage detection. Design a control system to minimize the effect of damage.

2. Accomplishments

A general framework has been developed for the analysis of laminated smart structures with embedded and/or surface bonded piezoelectric actuators and sensors. The theory addresses the following issues: (i) accurate description of transverse shear effects in the laminated structural model, (ii) presence of multiple delaminations and (iii) characterization of delamination placement and size on dynamic characteristics. The mathematical model has been implemented using finite element method and extensive numerical investigations have been performed to validate the model with three-dimensional results and available experimental data. Results indicate that the presence of delaminations affect the modal strain distributions in smart composite laminates. The developed theory has been used to characterize delaminations in smart composite plates of arbitrary thickness and results indicate that dynamic strain is a better indicator of damage than frequencies or mode shapes. Significant differences are noted in the RMS values of the response, calculated using modal strain, indicating the presence of damage. A control system has also been designed to minimize the effect of damage. New damage indices based on modal strain are proposed and show promising results.

3. Development of a Higher-Order Based Finite Element Model

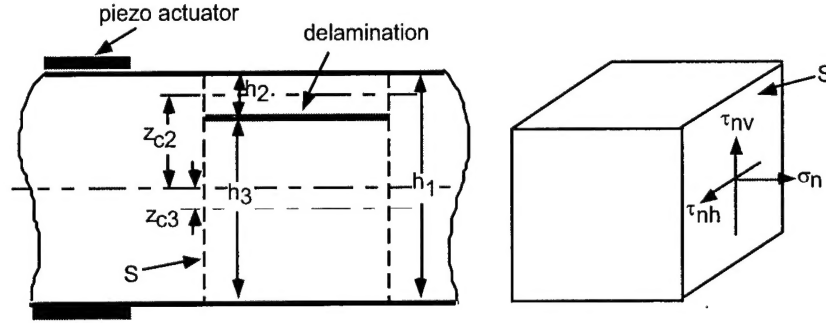


Fig. 1 Laminate cross section with delamination

The general higher order displacement field has been extended to model composite plates with surface bonded piezoelectric materials and delaminations (Fig. 1). The inplane displacements are effectively expressed by a cubic function through the thickness (z) and the transverse displacement is assumed to be independent of z . To model delamination in such structures, it is necessary to partition the laminate into several different regions as shown in Fig. 1. These regions include the undelaminated region, the region above the delamination, and the region below the delamination. The interface between the undelaminated region and the delaminated region, indicated by the dashed line in Fig. 1, is denoted S . The general form of the higher order displacement field is independently applied to each of these regions to describe displacements, which account for slipping and separation due to the delamination. The higher order displacement theory is used to model a composite laminate with multiple delaminations.

$$\begin{aligned} u_i(x, y, z, t) &= u_{0i}(x, y, t) + (z - z_{ci})[-w_{0i,x} + \alpha_i(x, y, t)] + (z - z_{ci})^2 u_{2i}(x, y, t) + (z - z_{ci})^3 u_{3i}(x, y, t) \\ v_i(x, y, z, t) &= v_{0i}(x, y, t) + (z - z_{ci})[-w_{0i,y} + \beta_i(x, y, t)] + (z - z_{ci})^2 v_{2i}(x, y, t) + (z - z_{ci})^3 v_{3i}(x, y, t) \\ w_i(x, y, z, t) &= w_{0i}(x, y, t) \end{aligned} \quad (1)$$

where u_i , v_i and w_i are the displacement functions, u_{0i} , v_{0i} and w_{0i} denote the midplane displacements of a point (x, y) , $w_{0i,x}$ and $w_{0i,y}$ represent the rotation of normals to the midplanes and α_i and β_i are the additional rotations due to shear deformation. The quantities u_{2i} , u_{3i} , v_{2i} and v_{3i} represent higher order functions. The index i is used to designate the three regions, $i=1$ the undelaminated region, $i=2$ the region above delamination and $i=3$ the region below delamination, while z_{ci} are the positions of the midplane for each region with respect to laminate midplane (Fig. 1) and t denotes time.

The transverse shear stresses, σ_4 and σ_5 , must vanish at all free surfaces, including at delamination interfaces. This leads to the following refined displacement field.

$$\begin{aligned} u_i(x, y, z, t) &= u_{0i}(x, y, t) + (z - z_{ci})[-w_{0i,x} + \alpha_i(x, y, t)] - 4(z - z_{ci})^3 \alpha_i(x, y, t)/(3h_i^2) \\ v_i(x, y, z, t) &= v_{0i}(x, y, t) + (z - z_{ci})[-w_{0i,y} + \beta_i(x, y, t)] - 4(z - z_{ci})^3 \beta_i(x, y, t)/(3h_i^2) \\ w_i(x, y, z, t) &= w_{0i}(x, y, t) \end{aligned} \quad (2)$$

In addition, continuity conditions of displacement and traction are imposed at the midplane points of each region on delamination lateral boundaries S (Fig. 1) as follows.

$$\begin{aligned} u_1(x, y, z_{ci}, t) &= u_i(x, y, z_{ci}, t) \\ v_1(x, y, z_{ci}, t) &= v_i(x, y, z_{ci}, t) \\ w_1(x, y, z_{ci}, t) &= w_i(x, y, z_{ci}, t) \end{aligned} \quad i = 2, 3 \quad (3)$$

and

$$\begin{aligned} \sigma_{n1}(x, y, z_{ci}, t) &= \sigma_{ni}(x, y, z_{ci}, t) \\ \tau_{nh1}(x, y, z_{ci}, t) &= \tau_{nhi}(x, y, z_{ci}, t) \\ \tau_{nv1}(x, y, z_{ci}, t) &= \tau_{nvi}(x, y, z_{ci}, t) \end{aligned} \quad i = 2, 3 \quad (4)$$

In the finite element formulation these continuity conditions are to be satisfied at the mesh node locations. The constitutive equations take the following vector-matrix form.

$$\mathbf{u}_S^i = \mathbf{T}^i \mathbf{u}_S^l \quad i = 2, 3 \quad (5)$$

where \mathbf{u}_S^i represents the generalized displacement vector in the regions above and below delamination, \mathbf{u}_S^l is the displacement vector in the undelaminated region and \mathbf{T}^i is the transformation matrix between regions.

In the context of laminated composite plates, the constitutive equations for the k^{th} laminae take the following form.

$$\boldsymbol{\sigma}_k = \mathbf{Q}_k \boldsymbol{\varepsilon}_k \quad (6)$$

where

$$\boldsymbol{\sigma}_k = [\sigma_x \quad \sigma_y \quad \tau_{yz} \quad \tau_{xz} \quad \tau_{xy}]_k^T \quad (7)$$

$$\boldsymbol{\varepsilon}_k = [\varepsilon_x \quad \varepsilon_y \quad \gamma_{yz} \quad \gamma_{xz} \quad \gamma_{xy}]_k^T \quad (8)$$

and

$$\mathbf{Q}_k = \begin{bmatrix} Q_{11} & Q_{12} & 0 & 0 & Q_{16} \\ Q_{12} & Q_{22} & 0 & 0 & Q_{26} \\ 0 & 0 & Q_{44} & Q_{45} & 0 \\ 0 & 0 & Q_{45} & Q_{55} & 0 \\ Q_{16} & Q_{26} & 0 & 0 & Q_{66} \end{bmatrix}_k \quad (9)$$

In the above equations, σ and ϵ denote the stress and the mechanical strain in the material coordinates respectively, \mathbf{Q} is the elastic stiffness matrix.

The finite element method is used to implement the theory. The equations of motion are derived using Hamilton's principle in the discrete form and can be written as follows.

$$\mathbf{M} \ddot{\mathbf{q}} + \mathbf{K} \mathbf{q} = \mathbf{F} \quad (10)$$

where \mathbf{M} , \mathbf{K} , \mathbf{F} and \mathbf{q} denote the mass matrix, the stiffness matrix, the force vector due to a distributed load and the nodal displacement vector, respectively. Bilinear shape functions are used for interpolating the inplane displacements u and v and rotations α and β while a 16 term cubic polynomial is used for the transverse displacement w . The representative four-noded element has 32 degrees of freedom.

Damage Detection and Vibration Control

To characterize the dynamic characteristics of smart composite plates, both delaminated and nondelaminated, are investigated next. The plate is subject to impulse and RMS values of the response are calculated in an attempt to understand the mechanics of damage detection. The equations of motion can be expressed as the following state equations.

$$\begin{aligned} \dot{\mathbf{X}} &= [\mathbf{A}] \{\mathbf{x}\} + [\mathbf{B}] \{\mathbf{u}\} + \{\mathbf{B}_w\} w \\ \mathbf{y} &= [\mathbf{C}] \{\mathbf{x}\} \end{aligned} \quad (11)$$

where $[\mathbf{A}]$, $[\mathbf{B}]$ and $[\mathbf{C}]$ are the state matrix, the control matrix and the output matrix respectively. The quantity w is white noise and $\{\mathbf{B}_w\}$ is noise vector. After vibration analysis, a modal reduction is performed using the first ten elastic modes. Therefore, the state matrix is of size (20×20). The RMS values of response for the elastic modes are obtained from the following equation.

$$\sigma_i^2 = [[\mathbf{C}][\mathbf{X}][\mathbf{C}]^T]_{ii}, i = 1, 2, \dots, N_s \quad (12)$$

where $[C]$ is the output matrix, $[X]$ is the state covariance matrix and N_s represents the number of structural states. The state covariance matrix $[X]$ of the system is the solution of a Lyapunov equation of the form

$$[A][X] + [X][A]^T + \{B_w\}Q_w\{B_w\}^T = 0 \quad (13)$$

where Q_w is the intensity of white noise. The RMS values of the elastic modes can be converted into displacement and velocity, at the nodal points, by multiplying the covariance matrix by the matrix Φ_2 as follows

$$\sigma_{q\dot{q}} = [\Phi_2 X \Phi_2^T]_{ii}, \quad \Phi_2 = \begin{bmatrix} \Phi & 0 \\ 0 & \Phi \end{bmatrix} \quad (14)$$

where $\sigma_{q\dot{q}}$ represents the RMS values of nodal displacement and nodal velocity and Φ is the eigenmatrix. The RMS values of the nodal displacements due to the disturbance are calculated for both the undelaminated and the delaminated plate models.

Active Control System Design to Minimize the Effect of Damage

The damage detection algorithm is extended to design an active control system. The goal is to reduce the RMS values and thereby minimize the effect of such damage. It is assumed that all states are available for feedback. The gain matrix of the completely controllable and observable linear dynamic system is expressed as follows

$$\{u\} = -[K_G]\{x\} \quad (15)$$

The right and left eigenvalue problems of the closed loop system can be written as

$$([A] - [B][K_G])\{\phi^c\}_i = \lambda_i^c \{\phi^c\}_i, \quad ([A] - [B][K_G])^T \{\psi^c\}_i = \lambda_i^c \{\psi^c\}_i \quad (16)$$

where $\{\phi^c\}_i$ and $\{\psi^c\}_i$ are the right and left eigenvectors of the closed loop system, respectively, corresponding to the eigenvalue λ_i^c .

The pole placement algorithm, based on Sylvester equation, utilizes the parameter vector defined by

$$\{h\}_i = [K_G]\{\phi^c\}_i \quad (17)$$

Substitution of Eq. (17) into Eq. (16) yields the following Sylvester equation

$$([A] - \lambda_i^c[I])\{\phi^c\}_i = [B]\{h\}_i \quad (18)$$

or in matrix form

$$[A][\Phi_c] - [\Phi_c][\Lambda_D] = [B][H] \quad (19)$$

where

$$\begin{aligned} [\Phi_c] &= [\{\phi^c\}_1, \{\phi^c\}_2, \dots, \{\phi^c\}_n] \\ [\Lambda_D] &= \text{Diag}(\lambda_1^c, \lambda_2^c, \dots, \lambda_n^c) \\ [H] &= [\{h\}_1, \{h\}_2, \dots, \{h\}_n] \end{aligned} \quad (20)$$

and $[\Lambda_D]$ contains the desired closed loop eigenvalues. From Eq. (18), it can be seen that

$$\{\phi^c\}_i = ([A] - \lambda_i^c[I])^{-1}[B]\{h\}_i \quad (21)$$

If λ_i^c are distinct from their open loop positions, the columns of $[H]$ generate the corresponding closed loop eigenvectors. For the given parameter matrix $[H]$, the closed loop modal matrix $[\Phi_c]$ can be determined by solving Sylvester equation. The gain matrix can be obtained from Eq. (17) as follows

$$[K_G] = [H][\Phi_c]^{-1} \quad (22)$$

Development of Damage Index

Finally, a new damage index is formulated using the difference between the inplane modal strains of the delaminated structure and those of a similar healthy structure. The difference in modal strains is squared to diminish the effects of numerical errors or experimental noise. This procedure requires an undamaged reference but is valid for any type of structure including smart laminate with stiffness discontinuity. The new damage index is defined as follows.

$$\delta_{ml} = \left[\varepsilon_{ml}^{rk} - (\varepsilon_{ml}^{rk})_{\text{del}} \right]^2 \quad (23)$$

where ml is the number of the element under investigation, r is the number of vibration mode for which the modal strain is computed and $k=1,2,6$ is the appropriate modal strain.

Results And Discussions

Results are presented for Graphite/Epoxy composite plates with five pairs of surface bonded piezoelectric actuators. The plates are clamped along one edge and other edges are free. The dynamic responses are investigated for plates with and without a small delamination (Fig. 3). The stacking sequence is $[0^\circ/0^\circ/90^\circ]_S$ and each ply has a uniform thickness of $0.0000134m$. The plate length is $0.305m$, width is $0.076m$ and total thickness is $0.000804m$. A delamination is placed at midplane in the region between $0.0152 < x < 0.0456$ m, $0.0305 < y < 0.061$ m. The material properties are: $E_1 = 98.0$ GPa, $E_2 = 7.9$ GPa, $\nu_{12} = 0.28$, $G_{12} = G_{13} = 5.6$ GPa, $G_{23} = 2.4$ GPa, $\rho = 1520$ Kg/m³ for the composite plate and $E = 63$ GPa, $\nu = 0.31$, $G = 24.2$ GPa, $\rho = 5000$ Kg/m³, $d_{12} = 250 \times 10^{-12}$ m/V for the piezoelectric material. Table 1 shows the effect of delamination on the first six natural frequencies of the composite plate. Some changes are observed in the values of the first three frequencies as a result of the small reduction in the structural stiffness due to delamination.

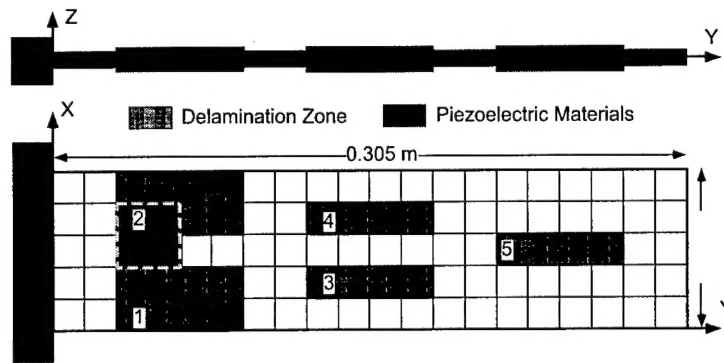


Fig. 2 Delaminated composite plate with piezoelectric actuators.

The RMS values of the nodal displacements due to the disturbance are calculated for both nondelaminated and delaminated plates. Figures 3 and 4 show the responses of the inplane displacement u , due to disturbance, for the nondelaminated and the delaminated plates, respectively. As seen from these figures, very significant differences are observed in the RMS values of inplane displacement between cases without and with delamination. In the presence of delamination, the

RMS values of the response due to disturbance increases, as shown in Fig. 4 compared to the nondelaminated plate (Fig. 3). This is once again due to the reduction in plate stiffness caused by the presence of delamination. Significant jumps in the RMS values in the delamination boundaries are also observed. This information can be used to identify delamination location and size. The RMS values of the out of plane displacement (w) were also calculated. However, it was found that the changes in RMS distributions of this displacement, between the delaminated and the nondelaminated plates, were not significant enough. Therefore, this information cannot be used to accurately capture the delamination zone.

	Nondel. Plate (Hz)	Del. Plate (Hz)
1	11.7	11.2
2	63.0	62.4
3	90.1	86.7
4	174	173
5	196	190
6	331	326

Table 1 Natural frequencies of nondelaminated and delaminated plates.

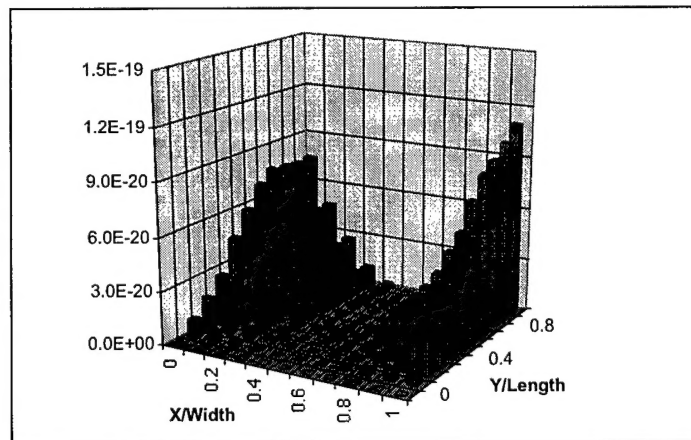


Fig. 3 RMS values of inplane displacement u , of nondelaminated plate.

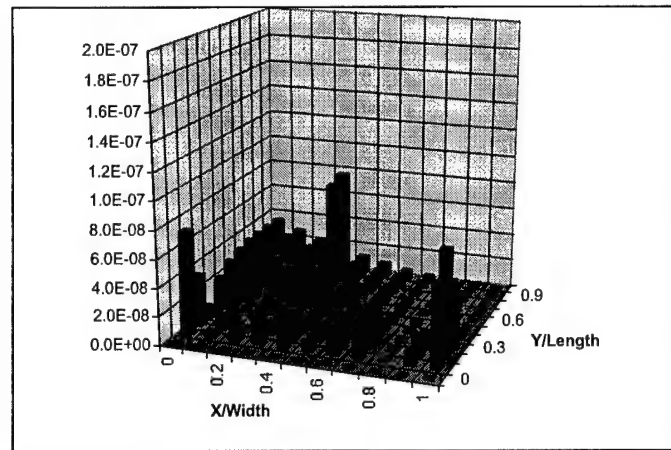


Fig. 4 RMS values of inplane displacement, u , of the delaminated plate.

Nondelaminated plate (open loop)	Delaminated plate (open loop)	Delaminated plate (closed loop)
$-.1475 \pm 73.77I$	$-.1410 \pm 70.51I$	$-7.377 \pm 73.77I$
$-.7921 \pm 396.7I$	$-.7843 \pm 392.1I$	$-39.60 \pm 396.0I$
$-1.131 \pm 565.9I$	$-1.089 \pm 544.8I$	$-56.59 \pm 565.9I$
$-2.190 \pm 1095.I$	$-2.176 \pm 1088.I$	$-109.5 \pm 1095.I$
$-2.463 \pm 1231.I$	$-2.390 \pm 1195.I$	$-123.1 \pm 1231.I$
$-4.162 \pm 2081.I$	$-4.106 \pm 2053.I$	$-208.1 \pm 2081.I$
$-4.986 \pm 2493.I$	$-4.906 \pm 2453.I$	$-249.3 \pm 2493.I$
$-5.673 \pm 2836.I$	$-5.606 \pm 2803.I$	$-283.6 \pm 2836.I$
$-6.357 \pm 3178.I$	$-6.094 \pm 3047.I$	$-317.8 \pm 3178.I$
$-6.395 \pm 3197.I$	$-6.380 \pm 3190.I$	$-319.7 \pm 3197.I$

Table 2 Changes in eigenvalues of the open loop and closed loop systems.

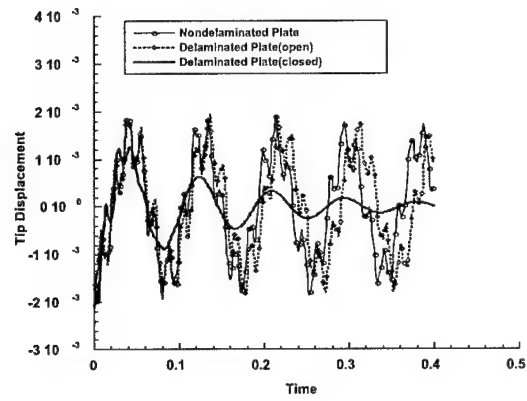
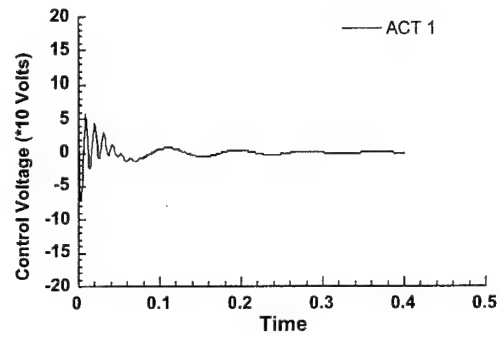
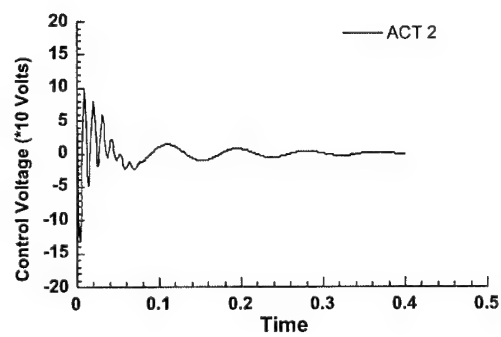


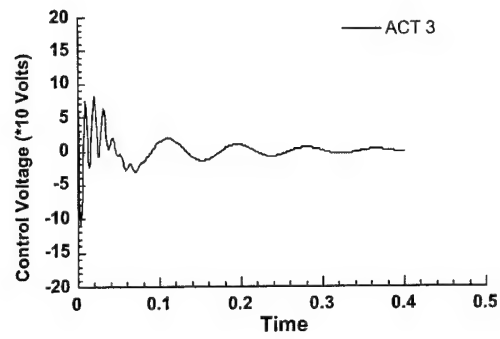
Fig. 5 Tip displacement of the composite plate due to disturbance.



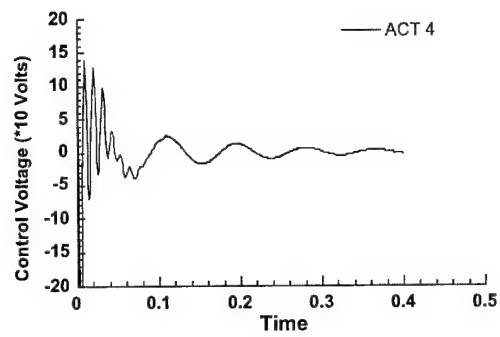
6(a)



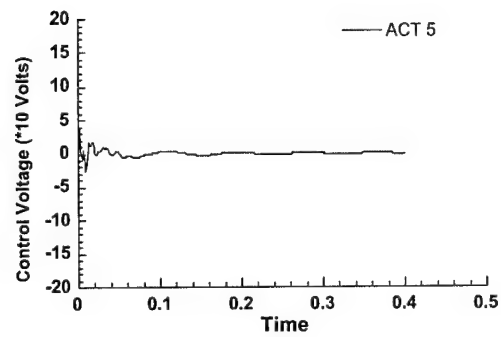
6 (b)



6 (c)



6 (d)



6(e)

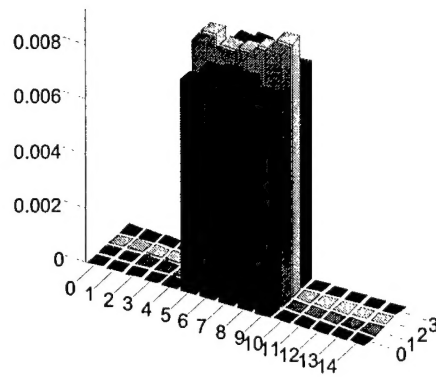
Fig. 6 Applied control voltage history.

Table 2 presents the changes in eigenvalues for both delaminated and nondelaminated plates with the application of the active control system. As seen from this Table, significant increases are observed in the real part of the closed loop eigenvalues for the delaminated plate. This indicates improved damping with closed loop control. The imaginary parts of the closed loop eigenvalues for the delaminated plate are almost identical to the corresponding open loop values for the nondelaminated plate. This implies that the natural frequencies of the two plates are almost identical. The RMS values of the first three elastic modes corresponding to the open loop system of the nondelaminated and delaminated plates are (15.227, 0.0292, 0.2093) and (21.035, 0.0142, 0.2578), respectively. With the application of the active control system, these values, for the delaminated plate, change to (0.681, 0.091, 0.0051). This indicates a very significant reduction (up to 78 percent) in the magnitude of the RMS values for the first and third modes. The RMS value of the second mode increases compared to the open loop case. However, the contribution of this mode is not significant enough to cause stability problem or degradation in the performance of the active control system. Therefore, the controller is successful in improving the dynamic characteristics of the delaminated plate.

To investigate the control performance of the designed system, the time histories of the tip displacement and the control voltages applied to the actuators are calculated. Figure 5 shows the time histories of the open loop and closed loop systems, due to disturbances, for the nondelaminated and the delaminated plates. The control system significantly improves the response of the delaminated plate compared to the nondelaminated plate (open loop). Figure 6 presents the control voltage applied to the actuators due to the disturbance. It can be seen that maximum applied voltage is less than 200 Volts implying no saturation effects.

Next, composite/smart composite plates with single or multiple delaminations are analyzed to verify the performances of the proposed damage indices. The geometry of the test structure consists of eight plies, each with thickness 1.27 mm and stacking sequence $[0^\circ/90^\circ/0^\circ/90^\circ]$. The material properties for the composite plate are the following, $E_1=134.4\text{GPa}$, $E_2=10.3\text{GPa}$, $\nu_{12}=0.33$, $G_{12}=G_{13}=5\text{GPa}$, $G_{23}=2\text{GPa}$ and $\rho=1477\text{Kg/m}^3$. First, a single delamination is introduced between the fourth and the fifth plies. The length of delamination is one third of the length of the plate. Next, two delaminations are symmetrically placed with respect to the plate edges. From Fig. 7, it can be observed that the proposed damage index

precisely indicates the delamination position and length, that is elements with $m=5-9$ and $l=1-4$. This damage index can be used in experimental work when the appropriate modal strain distribution is measured. Figure 8 presents the result of the damage index in the two-delamination case. It can be observed that the delaminated zone near the clamped end of the plate is precisely located. The elements with $m=3,4,5$ in the global mesh have a very high damage index compared to their neighbors. For the delamination placed near the free end, elements with $m=9,10$ are correctly indicated as belonging to the damaged zone. Therefore, this damage index is capable of identifying both delaminated zones quite accurately.



in

Fig. 7 Single delamination case

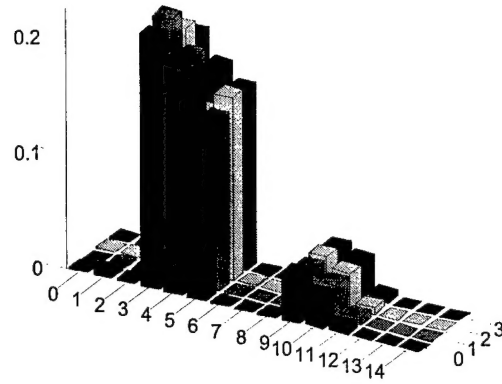


Fig. 8 Two delamination case.

Next, the delaminated composite laminate with piezoelectric patches is investigated as shown in Fig. 9. The dimension of the structure is of length $a=240\text{mm}$, width $b=135\text{mm}$ and total thickness of composite zone $h=3\text{mm}$. Four pairs of piezoelectric layers with length $L_p=75\text{mm}$, width $l_p=45\text{mm}$ and thickness $h_p=0.5\text{mm}$ are assumed to be bonded at the plate surface. The stacking sequence for this composite plate is $[90^\circ, 0^\circ, 45^\circ, -45^\circ, 0^\circ, 90^\circ]_s$. The same composite material is used and the piezoelectric material properties are: $E=63\text{GPa}$, $\nu=0.33$, $G=24.2\text{GPa}$, $\rho=7600\text{Kg/m}^3$ and $d_{12}=254 \times 10^{-12} \text{ m/V}$. Note that no electrical force is applied on the piezoelectric materials, therefore, electrical effects are not considered in the current study. In the delaminated case, a single through the width delamination of length $\beta=45\text{mm}$ is assumed to be placed between layers 7 and 8 of the composite plate. The numbering of layers starts with the bottom layer.

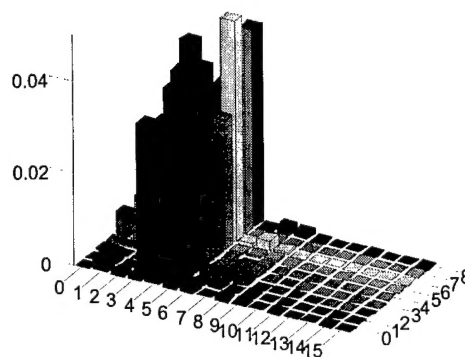


Fig. 9 Strain-based index (with delamination and actuators)

As seen from Fig. 9, the proposed strain-based index based is capable of identifying the position and extension of delamination quite accurately. The position corresponds to elements with numbers 3, 4 and 5 on x-axis. Indeed, elements with numbers 0, 1, 2 and 6-15, in the longitudinal direction, belong to either the healthy composite or active undamaged zones, while elements with numbers 3, 4 and 5 belong to top and bottom delaminated sublaminae.

Personnel Supported

Graduate Research Associate: Dan Dragomir-Daescu, Post-Doctoral Fellow: Dr. Haozhong Gu and Visiting Research Professor: Dr. Changho Nam

Publications (Archival Journal)

1. Chattopadhyay, A., Gu, H and Dragomir-Daescu, D., "Dynamics of Delaminated Composite Plates with Piezoelectric Actuators," *AIAA Journal*, Vol. 37, 2, 248-254, 1999.
2. Chattopadhyay, A., Li, J. and Gu, H., "Coupled Thermo-Piezoelectric-Mechanical model for Smart Composites," *AIAA Journal*, Vol. 37, 12, 1633-1638, 1999.
3. Chattopadhyay, A., Nam, C. and Dragomir-Daescu, D., "Delamination Modeling and Detection in Smart Composite Plates," *J. of Reinforced Plastics and Composites*, Vol 18, 17, 1557-1572, 1999
4. Nam, C., Chattopadhyay, A., and Kim, Y. H., "Optimal Wing Planform Design for Aerelastic Control," *AIAA Journal* Vol. 38, 8, 1465-1470, 2000.
5. Chattopadhyay, A., Nam, C. and Kim, Y., "Damage Detection And Vibration Control of a Delaminated Smart Composite Plate," *Advanced Composites Letters*, Vol. 9, 1, 2000, 7 - 15.

Discoveries/Inventions

The identification of damage through the use of dynamic strain and RMS values of the strain is unique in the field of structural health monitoring of heterogeneous smart systems. Conventional health monitoring studies rely on expensive experiments and crude analytical models. The findings from this research indicate that the accurate theory developed can be a useful tool in detecting the presence of delaminations in smart structures. Also, mode shapes, frequencies and curvature mode shapes are commonly used in formulating damage indices. The current research shows that dynamic strain is more effective in capturing the location and size of delamination in composites.

Honors/Awards

- Faculty Achievement Award - Excellence in Research, 2000, Arizona State University,
- Research citations, Adaptive Structures Highlight, *Aerospace America*, Year End Review, December 1998-2000.
- Research citations, Multidisciplinary Design Optimization Highlight, *Aerospace America*, Year End Review, December 1999.
- Research citations, Structures Highlight, *Aerospace America*, Year End Review, December 1998-2000